

Feel like an insect: a bio-inspired tactile sensor system

Sven Hellbach^{1,2}, André Frank Krause², and Volker Dürr^{1,2} *

¹ University of Bielefeld, Faculty of Biology, Dept. Biological Cybernetics,
² CITEC Center of Excellence Cognitive Interaction Technology
Universitätsstrasse 21-23, 33615 Bielefeld, Germany
<http://www.uni-bielefeld.de/biologie/Kybernetik/>
{sven.hellbach, andre_frank.krause, volker.duerr}@uni-bielefeld.de

Abstract. Insects use their antennae (feelers) as near range sensors for orientation, object localization and communication. This paper presents an approach for an active tactile sensor system. This includes a new type of hardware construction as well as a software implementation for interpreting the sensor readings. The discussed tactile sensor is able to detect an obstacle and its location in 3D space. Furthermore the material properties of the obstacles are classified by use of neural networks.

Key words: Active Tactile Sensing, FFT, Material Classification, Object Localization, Acceleration Measurement

1 Introduction

Insects are a widespread group of animals, inhabiting a wide range of ecosystems and hence being confronted with variate living conditions. One of the reasons why insects are able to adapt to such different living conditions is their ability for rapid and parallel object recognition and scene analysis. Researching the sensor systems of insects helps to understand the complexity of nature, since in animal near-range sensing, the active tactile sense is often of central importance. Many insects actively move their antennae (feelers) and use them for orientation, obstacle localisation, pattern recognition and even communication [1]; mammals like cats or rats use active whisker movements to detect and scan objects in the vicinity of their body. Here we use the antenna of the stick insect *Carausius morosus* [2] as the biological model for a bionic sensor for reasons summarised by Dürr and Krause [3]. This paper expands research efforts presented in [4] and some results are validated by application of a larger, hence more reliable data set. Furthermore, the algorithm is extended to provide even better results. While [4] can be seen as a proof of concept, this paper aims at a practical application.

Beyond the understanding of nature's principles, it offers a new type of sensor for mobile robot systems. In particular, in environments where other sensors are

* This work was supported by the German Research Council (DFG) DU380/3 and by the German ministry of research and education (BMBF) 0313766

not able to provide reliable data, e. g. vision sensors in dusty or dark environments, a tactile sensor is able to support such sensors by providing additional data. To stick with the example, it is difficult for vision sensors to determine material properties. The sensor described within this paper is able to provide information about the material with additional spacial information.

This paper presents two different methods for processing the sensor readings from the acceleration sensor. The first one is based on previous work in [4], where it could be shown that the derived method works well for estimating the contact position, and that it is able to classify two different kinds of material. Both was shown on a small data set for which the start and end of the contact was given. the known method has been improved to be able to deal with a continuous data flow, as well as to classify an arbitrary set of materials.

Furthermore, a second method is presented, which reduces the pre-processing steps by withdrawing some limiting constrains and allowing a neural network to find the necessary information within the data. In that way, better results for distance estimation are gained, especially for contact positions closer to the antennal tip.

The next section presents a short overview of the field of tactile sensing. The sensor hardware is introduced in section 3, while the software part is discussed in section 4. Afterwards, experimental results are presented in section 5. Finally, the work is concluded in section 6.

2 Previous Work

While thinking about scene understanding, particularly the understanding of scene objects, the use of tactile sensors in the broadest sense plays an increasing role [5, 6]. Insect-like tactile sensors have been pioneered by Kaneko and co-workers, who used either vibration signals [7] or bending forces [8], both measured at the base of a flexible beam, to determine contact distance. In contrast, we use a single acceleration sensor located at the tip of the probe [9]. Contact distance is determined using the peak frequency of the damped oscillations of the free end. Beyond the focus on single antenna-like sensors, their integration with vision has been researched, for example, in the AMouse project [10]. Instead of antennae rat inspired whiskers are used. Different to the approach in this paper the vibration is not measured at the tip of the sensor, but on its mounting point. In contrast to these works, our system is able to detect 3d contact position with a single antenna by measuring its vibration in two dimensions. The interpretation of the sensor readings is done in a bio-inspired way using neural networks.

3 Sensor Hardware

The biological counterpart is equipped with a large number of sensors. Handling such a large number of sensors is a challenging task. In particular, integrating all types of sensors into a single antenna-like device still is demanding. Here, we have decided to regard the antenna at a higher level of abstraction. One of

the basic features of the biological archetype is the ability to detect the position of potential obstacles and to analyse their properties. A first step to be able to mimic these abilities is to use a two axis acceleration sensor (Analog Devices ADXL210E), which measures the vibration characteristics during object contact. The used sensor is mounted at the tip of a 33 cm poly-acrylic tube. The antenna is designed in a way that the entire probing rod can be exchanged easily [4].

The robotic feeler was based on major morphological characteristics of the stick insect antenna, such as two rotary joints that are slanted against the vertical plane. The scale is approx. 10:1 compared to the stick insect to match that of the Bielefeld insectoid walking robot TARRY (Fig. 1). The actuator platform consists of two orthogonal axes. Two 6V DC motors (Faulhaber 1331T 006SR) were used rather than servo motors to minimise vibrations of the probe due to discrete acceleration steps. The linkage of the hinges was designed to mimic the action range of the stick insect, amounting to 90° vertical range, centred 10° above the horizon, and to 80° horizontal range centred 40° to the side. Positioning accuracy is limited by slack in the motors and amounts to approx. 5 mm at the tip of a 40 cm probe (approx. 7°).

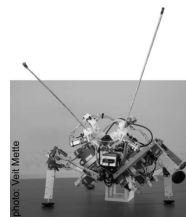


Fig. 1. The stick insect inspired walking robot TARRY

Both hinges are equipped with a position sensor (muRata SV01A). Hence the orientation of the sensor rod is known in two dimensions encoded in polar coordinates. Since the the hinge axes are orthogonal, no additional coordinate transformation is necessary. But, to describe the detected object's position in 3D space an additional coordinate is missing. It is gained by determining the contact position on the rod.

The control of the motion of the antenna as well as the sensor read out is implemented on an embedded system (ATMEL AT90CAN128). The raw sensor signal is available via RS232 for further processing.

4 Interpreting sensor readings

In the following two methods are described for the interpretation of the sensor signals. For both methods the principle idea stays the same. Depending on the position of contact, the free oscillating segment of the sensor tube differs. This results in different kinds of damped oscillations. Those characteristic properties of the damped oscillation are taken into account for estimating the position of contact. As an intuitive example, one can image a guitar string gripped at different position for playing different tone pitches.

In addition, the damped oscillation also carries information about the material involved. Back to the guitar string analogy this might be compared to the different tone caused by nylon or steel strings.

4.1 Method I: Constraint based input dimension reduction

The used acceleration sensor is able to measure the acceleration in two orthogonal dimensions. Hence, the data coming from the sensor is the projection of the

actual oscillation onto both dimension vectors. This leads to different sensor readings, depending on the rotation of the antenna with respect to the axis defined by it. To align the rotated oscillation with one of the axes PCA³ is applied. PCA computes a set of eigenvectors which are oriented with respect to the principle axes of the data distribution. The matrix of eigenvectors E can directly be used as an affine transform matrix applied on the data X : $X_{rotated} = E \cdot X$. The first dimension of the rotated data $X_{rotated}$ contains the part of the data with the largest variance. Only this part is used for further processing.

As a next step, it is necessary to know at which time a contact occurred. On a static system this is a trivial task, which can be solved with a simple threshold. However, it becomes more challenging while the active tactile sensor is in motion, since the motion induces an oscillation into the sensor rod as well. At the moment we stick to the threshold, keeping in mind that our further research will focus on that problem. For detecting the end of the oscillation the local maxima over time are considered. The end point is defined as the time, at which these maxima begin to drop below a dynamic threshold. The threshold is chosen to be 10% of the global maximum of the current damped oscillation. The window from the detected start to end point is taken into account for further processing after removing the mean.

As described above the basic idea is to take into account the frequency characteristics of the damped oscillation. Hence, the frequency spectrum of the time series within the window is computed using Discrete Fourier Transform.

Distance Estimation: Assuming that the fundamental oscillation and first harmonics are represented as significant peaks in the spectrum, two local maxima are determined. In doing so, the spectrum is divided into two intervals defined by the maximal and minimal occurring frequencies defined by the lengths of the rod. The intervals are chosen to be (0Hz, 55Hz] and (55Hz, 250Hz]. For each of the intervals their global maximum is derived, assuming to represent the fundamental oscillation and first harmonics respectively. Both values are presented as input to a multi-layer perceptron. The network is a standard 2-layered network with a sigmoidal output function in the hidden layer and a linear function in the output layer using the Levenberg-Marquardt algorithm for training.

Material Classification: For material classification, the extracted frequencies used for distance estimation are not sufficient. Different material properties result in different decay characteristics of the damped oscillation. To extract these characteristics reliably for the fundamental oscillation and first harmonic, we remove disturbing frequencies first. For this, we apply two bandpass filters with the same limits as the already discussed intervals: (0Hz, 55Hz] and (55Hz, 250Hz]. Both filtered spectra are transferred back into time domain. This results in two damped oscillation with different frequency and decay rate. For both, all local maxima are identified and an exponential decay function is fit:

$$f(t) = p_{0,j} + p_{1,j} \cdot e^{-\frac{t}{p_{2,j}} + p_{3,j}} \quad (1)$$

³ principle component analysis

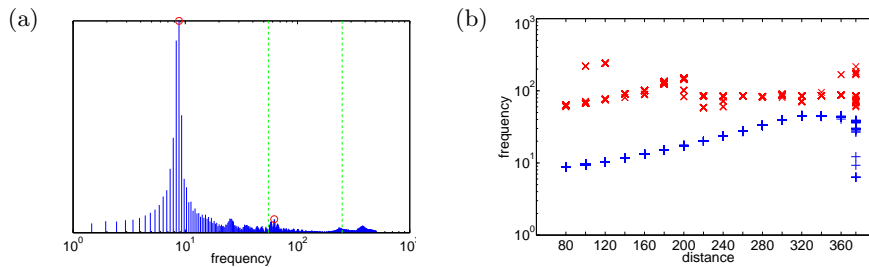


Fig. 2. (a) An example for a frequency spectrum of the damped oscillation caused by hitting an obstacle. Two dashed vertical lines indicate the intervals for the maximum frequency search. The circles show the position of the fundamental oscillation and the first harmonics. (b) The relation between the contact distance and the fundamental oscillation (+) and the first harmonics (\times) is shown.

where $p_{0,j}$ to $p_{3,j}$ denote offset, amplitude, time constant and delay, respectively, computed for each of the filtered oscillations $j \in \{0, 1\}$. Those 8 parameters together with the extracted frequencies of the fundamental oscillation and the first harmonics are used as input for the neural classifier. As shown in [4], the parameters of the decay function not only depend on the material property but also on the position of contact. By also providing the two extracted frequencies, the neural network is able to derive the necessary information.

4.2 Method II: Let the neural network do the work

For the second method, the pre-processing doesn't go further as to calculate the frequency spectrum. So, as well as for method I, the data is aligned using PCA and the start and end point are derived. However, neither the search for the significant peaks nor the exponential fit are calculated.

Instead of using only a two dimensional input vector for distance estimation as it is done in method I, the network for method II gets a much higher dimensional input vector involving the entire spectrum. Experiments show that a sub-sampled spectrum is sufficient to learn the mapping, reducing the number of input dimensions. However, the network has to learn which part of the spectrum is important to solve the distance estimation task. It is clear that the mapping is more complex than for method I and thus a larger network is necessary. The network showing best results is a 3-layer network with 20 neurons for the first hidden layer and 5 for the second one.

Unlike method I, the input for material classification is the same as for the distance estimation task. The network as well is a multi-layer perceptron with 20, 30, and 30 neurons for the 3 hidden layers.

5 Results

The experiments show, that the active tactile sensor is able to discriminate different types of material as well as to derive the position of contact. Hence, six

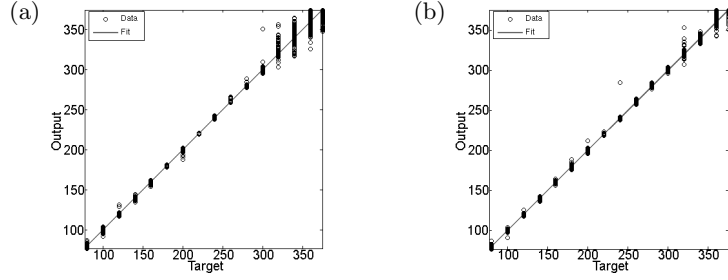


Fig. 3. Both plots show a regression plot, which indicates the relation between the network output distance and the desired target distance (both in mm). Each data sample is represented as a circle. An optimal solution would be located on the bisectrix $y = x$. Figure (a) shows the results for method I possessing larger errors for positions near the tip ($d > 300$) compared to the results of method II in Figure (b).

cylindrical objects with identical diameter were presented to the sensor, consisting of different materials, namely aluminium, wood, copper, brass, POM⁴, and acrylic glass. These materials were chosen to represent a wide spectrum of materials with different damping characteristics. The selection includes such that are expected to be discriminated easily, e. g. aluminium and wood, as well as such that are much harder to distinguish, e.g. the two kinds of plastic. The impact occurred at 16 positions along the sensor tube, at 80mm to 360mm in steps of 20mm and at 375mm, as measured from the centre of rotation. Each impact was repeated 100 times to provide a large data set for network training.

In order to test the optimal performance of the of the active tactile sensor, the experiments in this paper are limited to a stationary case, i. e. all used data sets are recorded with a stationary antenna. To do so, the antenna was mounted on a working desk with the objects to be probed fixed in the desired distance. The contact at different distances always occurred with the same angle of impact. In the experiments presented here, the algorithm controlling the movement of the antenna ensures that the antenna stops and keeps applying a constant pressure to the probe, as soon as the probe has been hit. The application a constant pressure is necessary to avoid the rebounding of the antenna.

The curve in Figure 2 suggests that the first harmonics (\times) can not be used any more from a distance of 200mm onwards. Even the fundamental oscillation ($+$) flattens for distant contacts. Since the network has to find a mapping from frequency values to distance (which is the inverse function to one being plotted). Performance is expected to deteriorate for contact distances beyond 300 mm. This can be confirmed in the regression plot in Figure 3. The network performance results in a root mean squared error (rmse) of 2.93 (about 0.7% of the antenna length). In contrast, when using the entire spectrum instead of the extracted frequencies performance improves to a rmse of 1.71. As a confirmation, whether this effect is not due to the changed network size, only the lower

⁴ polyoxymethylene

		Target Class							
		Aluminium	Wood	Copper	Brass	POM	Acrylic glass		
Output Class	Aluminium	770	0	1	2	1	36	95.1%	4.9%
	Wood	1	639	39	63	68	4	78.5%	21.5%
	Copper	3	19	732	20	12	15	91.4%	8.6%
	Brass	1	69	19	687	20	29	83.3%	16.7%
	POM	1	73	7	28	699	0	86.5%	13.5%
	Acrylic glass	24	0	2	0	0	716	96.5%	3.5%
		96.3%	79.9%	91.5%	85.9%	87.4%	89.5%	88.4%	
		3.8%	20.1%	8.5%	14.1%	12.6%	10.5%	11.6%	
		Target Class							
		Aluminium	Wood	Copper	Brass	POM	Acrylic glass		
Output Class	Aluminium	1448	10	5	9	2	22	96.8%	3.2%
	Wood	11	1414	61	80	45	6	87.4%	12.6%
	Copper	15	56	1441	80	21	5	89.1%	10.9%
	Brass	16	62	72	1384	32	11	87.8%	12.2%
	POM	46	42	16	38	1496	4	91.1%	8.9%
	Acrylic glass	64	16	5	9	4	1552	94.1%	5.9%
		90.5%	88.4%	90.1%	86.5%	93.5%	97.0%	91.0%	
		9.5%	11.6%	9.9%	13.5%	6.5%	3.0%	9.0%	

Fig. 4. Confusion Matrix for material classification: The matrix summarizes the number of data samples assigned to a specific class by the network (output class) broken down into their target classes. The diagonal entries (light grey) contains number of the true positive classifications. The border columns and rows (dark grey) indicate the percentage of the correct and incorrect classified elements per class, while entries in the lower right right corner tells the overall performance. Figure (a) shows the results for method I and (b) for method II.

band of the spectrum serves as input. The results are comparable with the ones with extensive pre-processing. This can be explained by the fact that the upper part of the spectrum provides redundant information which makes the decision process more robust.

Furthermore, instead of using the entire spectrum a sub-sampled spectrum containing only each 10th frequency used as input. The classification results were not different from the ones using the entire spectrum, but the calculation time for training was 5 times faster (340 min vs. 79 min under MatLab on a Intel Core2Duo E8500).

In contrast to the experiments presented in [4] the material classification is performed with more than two materials and at different contact positions. The only restriction for the experiments on method I (Figure 4(a)) is to use only measurements up to 240 mm. This is done to avoid similar difficulties as for distance estimation and to focus on the limits of material classification. Experiments show that adding trials with larger distance leads to worse results and unstable convergence. In contrast, method II (Figure 4(b)) is able to handle distances larger than 240 mm and even to obtain better results than method I. However, when applying the same restrictions as for method I the results become even better (97.2% correct classified trials).

6 Conclusion

In this paper, a bio-inspired tactile sensor was presented. The system is able to detect the position of a possible obstacle and is furthermore able to classify its material properties. We were able to extend the method presented in [4]. Beyond this, a second method was introduced which leads to better results.

Experiments show that, if the contact position is close to the tip, both distance estimation and material estimation are less reliable. To cope with this limitation for a practical application, the search and detection strategy could be designed in an adequate way. This could be done, for example, by positioning the

robot after the first contact in a way that for the second contact the expected contact position is below the critical distance.

However, before being able to include the antenna into a mobile robot, it is necessary to extend the pre-processing algorithm in a way that is able to handle self-induced noise by the motion of the robot.

Furthermore using only a tenth of the spectrum can be regarded as a first proof of concept. A deeper study on which part of the spectrum is sufficient, needs further investigations.

In this paper only simple multi-layer perceptrons were applied. Nevertheless, the data being processed is data with temporal characteristics, what suggests to apply recurrent neural network. Using recurrent networks would help to eliminate the start/stop-detection, which is done as the first pre-processing step. In that way distance estimation and material classification could run in an on-line system.

As a further perspective, it is desired to integrate multiple sensors onto a mobile platform. In doing so, a monocular vision-based system would benefit from the additional use of tactile sensors. The hypotheses gained from the vision system could be augmented with further information, like the detected material or the object's exact location in 3D Cartesian space. Additionally, the system is able to verify the visual object detection hypotheses.

References

1. Staudacher, E., Gebhardt, M., Dürr, V.: Antennal movements and mechanoreception: neurobiology of active tactile sensors. *Adv. Insect Physiol.* **32** (2005) 49–205
2. Dürr, V., König, Y., Kittmann, R.: The antennal motor system of the stick insect *Carausius morosus*: anatomy and antennal movement pattern during walking. *J. Comp. Physiol. A* **187** (2001) 31–144
3. Dürr, V., Krause, A.: The stick insect antenna as a biological paragon for an actively moved tactile probe for obstacle detection. In: *Proc. of CLAWAR 2001.* (2001) 87–96
4. Dürr, V., Krause, A.F., Neitzel, M., Lange, O., Reimann, B.: Bionic Tactile Sensor for Near-Range Search, Localisation and Material Classification. In: *AMS.* (2007) 240–246
5. Bebek, O., Cavusoglu, M.C.: Whisker sensor design for three dimensional position measurement in robotic assisted beating heart surgery. In: *IEEE ICRA, Roma, Italy.* (2007) 225–231
6. Kaneko, M., Kanayama, N., Tsuji, T.: Vision-based active sensor using a flexible beam. In: *IEEE-ASME Trans Mechatronics I. Volume 6.* (2001) 7–16
7. Ueno, N., Svinin, M.M., Kaneko, M.: Dynamic contact sensing by flexible beam. *IEEE-ASME Trans. Mechatronics* **3** (1998) 254–264
8. Kaneko, M., Kanayama, N., Tsuji, T.: Active antenna for contact sensing. *IEEE Trans. Robot. Autom.* **14** (1998) 278–291
9. Lange, O., Reimann, B., Saenz, J., Dürr, V., Elkmann, N.: Insectoid obstacle detection based on an active tactile approach. In: *Proc. of AMAM.* (2005)
10. Fend, M., Bovet, S., Hafner, V.: The artificial mouse - A robot with whiskers and vision. In: *Proc. of the 35th ISR.* (2004)